The *Drosophila* F-box protein Archipelago controls levels of the Trachealess transcription factor in the embryonic tracheal system

Nathan T. Mortimer, Kenneth H. Moberg *

Department of Cell Biology, Emory University School of Medicine, 615 Michael St. WBRB 442, Atlanta, GA 30322, USA

Abstract

The *archipelago* gene (*ago*) encodes the F-box specificity subunit of an SCF(*skp*-*c*ullin-*f* box) ubiquitin ligase that inhibits cell proliferation in *Drosophila melanogaster* and suppresses tumorigenesis in mammals. *ago* limits mitotic activity by targeting cell cycle and cell growth proteins for ubiquitin-dependent degradation, but the diverse developmental roles of other F-box proteins suggests that it is likely to have additional protein targets. Here we show that *ago* is required for the post-mitotic shaping of the *Drosophila* embryonic tracheal system, and that it acts in this tissue by targeting the Trachealess (Trh) protein, a conserved bHLH-PAS transcription factor. *ago* restricts Trh levels in vivo and antagonizes transcription of the *breathless* FGF receptor, a known target of Trh in the tracheal system. At a molecular level, the Ago protein binds Trh and is required for proteasome-dependent elimination of Trh in response to expression of the Dysfusion protein. *ago* mutations that elevate Trh levels in vivo are defective in binding forms of Trh found in Dysfusion-positive cells. These data identify a novel function for the *ago* ubiquitin-ligase in tracheal morphogenesis via Trh and its target *breathless*, and suggest that *ago* has distinct functions in mitotic and post-mitotic cells that influence its role in development and disease.
© 2007 Elsevier Inc. All rights reserved.

Keywords: Drosophila; Tracheal development; Degradation; F-box; Trachealess; Fbw7

Introduction

The morphogenesis of branched networks of cells with a single, fused lumen plays an important role in the development of many metazoan organs, including the vertebrate lungs, vasculature, kidneys, and mammary glands. The cellular architecture of these mammalian organs is quite similar to tubular structures in simpler metazoans, suggesting that the molecular and cellular mechanisms underlying the process of branching morphogenesis are conserved. In the fruit fly *Drosophila melanogaster*, tubular morphogenesis underlies formation of the tracheal system, a network of interconnected tubes that duct air throughout the developing organism. The complete embryonic tracheal network is composed of approximately 1600 polarized epithelial cells that originate in early embryogenesis as 20 ectodermal placodes distributed along either side

of the embryo (Samakovlis et al., 1996). Each tracheal placode contains approximately 20 cells, which undergo two rounds of cell division, exit the cell cycle, and complete the subsequent stages of invagination and tracheogenesis without further cell division or cell death. Following invagination, primary branches bud from the tracheal sac and form a continuous lumen within each placode (Lubarsky and Krasnow, 2003). The pattern of placode branching is segmentally repeated and under fixed genetic control (Samakovlis et al., 1996). Budded branches extend toward their target tissues by a process of cell migration and cell extension, and subsequent fusion between adjacent tracheal metameres at later stages of embryogenesis produces a continuous, open tubular system.

Forward genetic screens for mutations that disrupt tracheal development have revealed a central role for fibroblast growth factor (FGF) signaling in promoting the post-mitotic cell migration and extension of the embryonic tracheal arbor (reviewed in Metzger and Krasnow, 1999). The central components of the *Drosophila* FGF pathway are encoded by the *breathless* (*btl*) (Klambt et al., 1992) and *branchless* (*bnl*)

* Corresponding author.
  E-mail address: kmoberg@cellbio.emory.edu (K.H. Moberg).

(Sutherland et al., 1996) genes, which encode an FGF-like receptor and an FGF-like secreted ligand respectively. The role of this receptor/ligand pair in controlling tracheal outgrowth is based upon a simple model in which the restricted expression of *bnl* in cells outside the tracheal placode represents a directional cue for the migration of *btl*-expressing cells within the tracheal placode. Initial induction of *btl* transcription within tracheal cells depends upon the *trachealess* (*trh*) gene, which encodes a basic helix–loop–helix Per/Arnt/Sim (bHLH-PAS) domain transcription factor (Isaac and Andrew, 1996; Kuo et al., 1996; Ohshiro and Saigo, 1997; Wilk et al., 1996) most closely homologous to the mammalian NPAS1 and NPAS3 proteins (Brunskill et al., 1999; Zhou et al., 1997). Mutation of any one of these core components – *btl*, *bnl*, or *trh* – produces a failure of tracheal branching. Phenotypic analysis of these and other tracheogenesis genes has shown that Btl/FGF signaling is used to promote successive rounds of primary and secondary tracheal branching during embryonic *Drosophila* development (reviewed in Ghabrial et al., 2003). A similar role has been proposed for the FGF pathway in controlling the branching morphogenesis of tubes in the mammalian lung (Min et al., 1998).

In addition to a positive role in tracheal outgrowth, experimental evidence indicates that inappropriately timed Btl/FGF signaling can also impair tracheal development. First, in the course of normal development *btl* expression is not constant in tracheal cells, but oscillates: initially *btl* mRNA rises in all placode cells at stages 10–12 preceding primary branch formation, subsequently falls during late stage 12/early stage 13, and is re-initiated in a restricted set of cells that define sites of secondary branching at late stage 13/early stage14. Unlike early *btl* expression, this second wave is dependent upon a *bnl*-dependent feedback loop (Ohshiro et al., 2002; Ohshiro and Saigo, 1997). Second, ectopic activation of Btl, either by mutational inactivation of the *btl* inhibitor *abnormal wing disc* (*awd*) (Dammai et al., 2003), or by constitutive expression of *bnl* (Sutherland et al., 1996) or *btl* (this study and Lee et al., 1996), interferes with directed cell migration in the trachea. Similarly, expression of activated Ras or *btl* perturbs the ability of tracheal cells to form proper branching patterns in larval development (Cabernard and Affolter, 2005). These observations have led to the hypothesis that spatial and quantitative restriction of Btl activity is necessary to permit normal patterns of tracheal cell migration and fusion (Lee et al., 1996). While many genes that modulate Btl/FGF signaling have been identified, it is likely that other as yet unrecognized mechanisms are required to restrict Btl/FGF signaling to specific times and places in the developing organism.

Here we identify *archipelago* (*ago*), a gene known primarily for its role in cell proliferation control, as a component of the genetic circuitry that patterns the post-mitotic development of the embryonic tracheal system. *ago* encodes an F-box/WD-repeat protein that recruits target proteins to an SCF-type E3 Ub-ligase for subsequent poly-ubiquitination and proteolytic destruction. *ago* limits the division and growth of *Drosophila* eye epithelial cells by targeting the G1/S regulator Cyclin E and

dMyc, the fruit fly ortholog of the human c-Myc proto-oncogene, for proteasome-mediated degradation (Moberg et al., 2001, 2004). A highly conserved mammalian *ago* ortholog (variously termed Fbw7, Fbxw7, hAgo, hCDC4, or hSel-10) also targets Cyclin E and c-Myc and is a mutational target in a rapidly expanding array of human cancers (Balakrishnan et al., 2007; Bredel et al., 2005; Calhoun et al., 2003; Hagedorn et al., 2007; Malyukova et al., 2007; Mao et al., 2004; Maser et al., 2007; Minella et al., 2007; O'Neil et al., 2007; Rajagopalan et al., 2004; Thompson et al., 2007). Our current data indicate that *ago* is required for tracheal morphogenesis via a previously unrecognized target, the Tracheales (Trh) transcription factor. We find that *ago* mutant embryos contain excess Trh protein and ectopically express the *btl* gene, a known Trh target. Alleles of *ago* exhibit strong genetic interactions with *trh* and other known tracheogenesis genes, and the Ago protein is able to bind the Trh protein and regulate its proteasomal turnover via a mechanism that involves a third factor, the bHLH-PAS protein Dysfusion (Dys; Jiang and Crews, 2003). Collectively, these data reveal a previously unappreciated developmental function for the *ago* tumor suppressor in the embryonic tracheal system, and identify the Trh transcription factor as a target of Ago in this process.

Materials and methods

Stocks, genetics, and statistics

The *ago* alleles ago^1 and ago^3 have been previously described (Moberg et al., 2001). Unless indicated, analysis was performed on ago^1/ago^3 trans-heterozygotes. Full-length *ago* and *agoΔF*, a version of *ago* lacking the core F-box domain (Moberg et al., 2004), were cloned as PCR products into the *Eco*RI site of the *pUAST* vector (Brand and Perrimon, 1993) and used to generate *UAS-ago* and *UAS-agoΔF* stocks (D. Rennie, Massachusetts General Hospital Transgenic Drosophila Core). Other alleles used in this study were: btl^{dev1}, $btl^{EY01638}$, trh^{10512}, awd^{J2A4}, *Df(3L)Exel9000* and *esg-lacZ* (all from Bloomington Drosophila Stock Center), *1-eve-1* (Perrimon et al., 1991), *btl-Gal4* (Shiga et al., 1996), *UAS-trh* (Jin et al., 2001), *FRT80B, UAS-CycE, UAS-dMyc*. Crosses involving the temperature-sensitive $UAS-Pros26^1$ and $UAS-Prosβ2^1$ transgenes (gift of J. Belote) were performed at 21 °C. Embryos were genotyped using the *TM6B, P{iab-2(1.7)lacZ}6B, Tb^1* and *CyO, P{elav-lacZ.H}YH2* 'blue' balancers, or the *TM3, P{Gal4-twi.G}2.3, P{UAS-2xEGFP}AH2.3, Sb^{1}Ser^1* balancer. Statistical comparisons were made using Student's *t*-test.

Embryo immunohistochemistry and antibodies

Embryos were staged and fixed in 37% formaldehyde-saturated heptane, devitellinized in methanol and stored in ethanol at 4 °C. These samples were rehydrated and washed in PBS with 0.05% Triton-X 100 (PBSTx), blocked in 5% milk powder/5% NGS in PBSTx, and incubated with the following primary antibodies: mouse anti-Tango (1:5, Developmental Studies Hybridoma Bank; DSHB), rat anti-Trh (1:200) a gift of D. Andrew (Henderson et al., 1999), mouse mAb2A12 (1:5; DSHB), rabbit anti-β-Gal (1:300; Cappel), guinea pig anti-full length Ago (1:2500; Pocono Rabbit Farm & Laboratory), rat anti-Dys (1:200) and rabbit anti-Dys (1:800) both a gift of S. Crews (Jiang and Crews, 2003). Secondary antibodies conjugated to HRP, AP, Cy3, and Cy5 were used as recommended (Jackson ImmunoResearch). Embryos from w^{1118} and *ago^1/TM3, P{Gal4-twi.G}2.3, P{UAS-2xEGFP}AH2.3, Sb^{1}Ser^1* strains were collected at stages 13/14 and sorted by absence of GFP fluorescence. Extracts were prepared in sample buffer containing DTT and resolved on 7.5% SDS-PAGE prior to Western blotting with rat anti-Trh (1:2000), or anti-β-tubulin (1:2000; Santa Cruz Biotechnology). Anti-HA and anti-Flag antibodies (Sigma) were used according to manufacturer's instructions.

RNA analysis

RNA in situ hybridization was performed as described (Tautz, 2000). Briefly, embryos were fixed in 1.5% formaldehyde (in 0.1 M HEPES, pH 6.9, 2 mM MgSO$_4$, 1 mM EGTA)-saturated heptane, devitellinized, and stored in methanol at −20 °C. Embryos were washed in PBS with 0.1% Tween 20, treated with 15 μg/ml Proteinase K for 2 min, and post-fixed with 4% paraformaldehyde. Riboprobe hybridization and subsequent immunohistochemistry were performed as described (Tautz, 2000). Sense and anti-sense digoxigenin (DIG)-labeled riboprobes were synthesized from a 1 kb PCR fragment amplified from *btl* cDNA and visualized by the anti-DIG-AP antibody (1:2000; Roche).

Plasmids and molecular biology

pMT-HA-ago expression plasmids have been described previously (Moberg et al., 2004). *pMT-Flag-trh* was generated by cloning the full-length *trh* ORF (Open Biosystems) into the *pMT* vector as an N-terminally Flag-tagged PCR product. The *pACT-HA-dys* plasmid (gift of S. Crews) contains an N-terminally tagged version of the *dys* ORF under the control of a constitutively active fragment of the *actin* promoter. Transfected S2 cells were induced by the addition of 0.5 mM CuSO$_4$ for 6 h prior lysis in buffer containing 0.5M KCl, 0.1% NP-40, 35% glycerol, 10 mM HEPES pH 7.0, 5 mM MgCl$_2$, 0.5 mM EDTA pH 8.0, 25 mM NaF, 1 mM Na$_2$VO$_4$, 1 mM DTT supplemented with protease inhibitors (Complete™ Protease Inhibitor Cocktail; Roche). Where indicated, 50 μM MG132 (Calbiochem) was added 6 h prior to harvesting cells. Lysates were analyzed directly by immunoblot (IB), or diluted in immunoprecipitation (IP) buffer and subject to IP/IB analysis as described previously (Moberg et al., 2004).

Results

ago has role in embryonic tracheal development

Analysis of the growth restrictive role of *ago* in proliferating larval imaginal disc cells has provided an excellent model to understand the tumor suppressive properties of *ago* mammalian

Table 1
ago^1 and *ago^3* behave as null alleles in tracheogenesis

Genotype	DT breaks (%)	n=
FRT80B	3 [a]	61
ago^1/ago^3	46	85
ago^1/Exel9000	39	57
ago^3/Exel9000	38	42

Percent penetrance of the dorsal trunk 'break' phenotype in embryos of the indicated genotypes.
[a] $p<0.01$ compared to *ago$^{1/3}$*.

orthologs. However, the Ago protein is widely expressed in the early embryo (Fig. 1) and mutations that disrupt it lead to embryonic death (Moberg et al., 2001). Intercrossing the *ago^1* or *ago^3* alleles (respectively encoding a C-terminal truncation in the WD-repeat/substrate-binding domain and a G1131E missense mutation in the 4th WD repeat; Moberg et al., 2001) produces *trans*-heterozygous mutant embryos that develop through all embryonic stages but fail to hatch as L1 larvae (data not shown), suggesting lethality occurs during late embryogenesis. The severity of this and other phenotypes (see below) in homozygous or heteroallelic mutant animals is indistinguishable from those carrying either allele *in trans* to a chromosomal deficiency that removes the *ago* locus (Table 1; *Df(3L) Exel9000*), indicating that *ago^1* and *ago^3* are either null or strong loss-of-function alleles. Considered together, these observations indicate that *ago* may have as yet unappreciated roles in early development.

The earliest morphological defects in *ago* zygotic mutant embryos are observed in the developing trachea visualized with the anti-lumen antibody mAb2A12 (Figs. 2C–F). This analysis reveals two major defects in tracheal branching patterns of *ago*
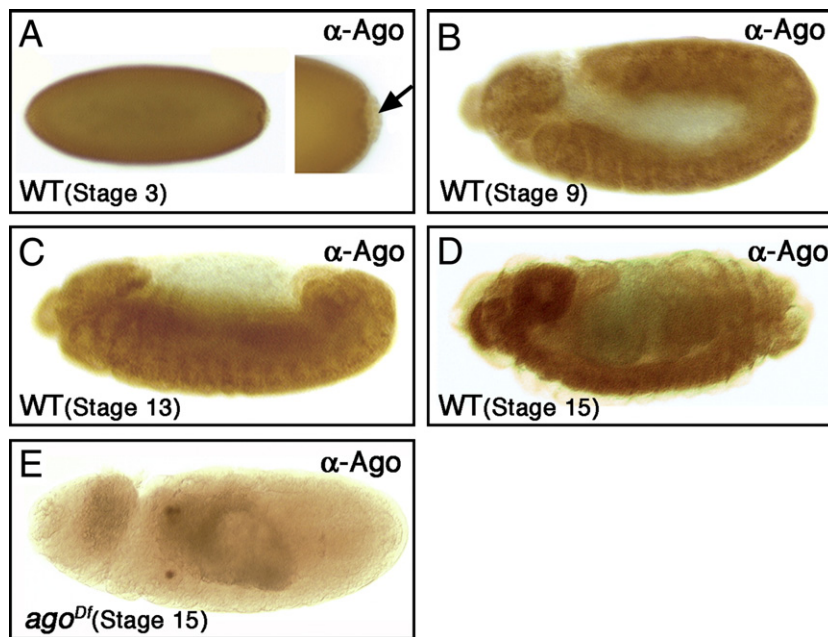

Fig. 1. Ago is widely expressed during embryogenesis. Lateral views of *FRT80B* control embryos stained with Ago-specific antiserum. Ago expression is detected uniformly during the cellularization (A), and germ-band extended (B) and retracted (C) stages, but is not detectable in pole cells (arrow in panel A). Ago is concentrated in the CNS during late embryogenesis (D). In this and all further figures, embryos are shown anterior left and dorsal up (unless indicated). Anti-Ago staining in an embryo homozygous for the *Df(3L)Exel9000* deletion, which removes the *ago* gene (E).
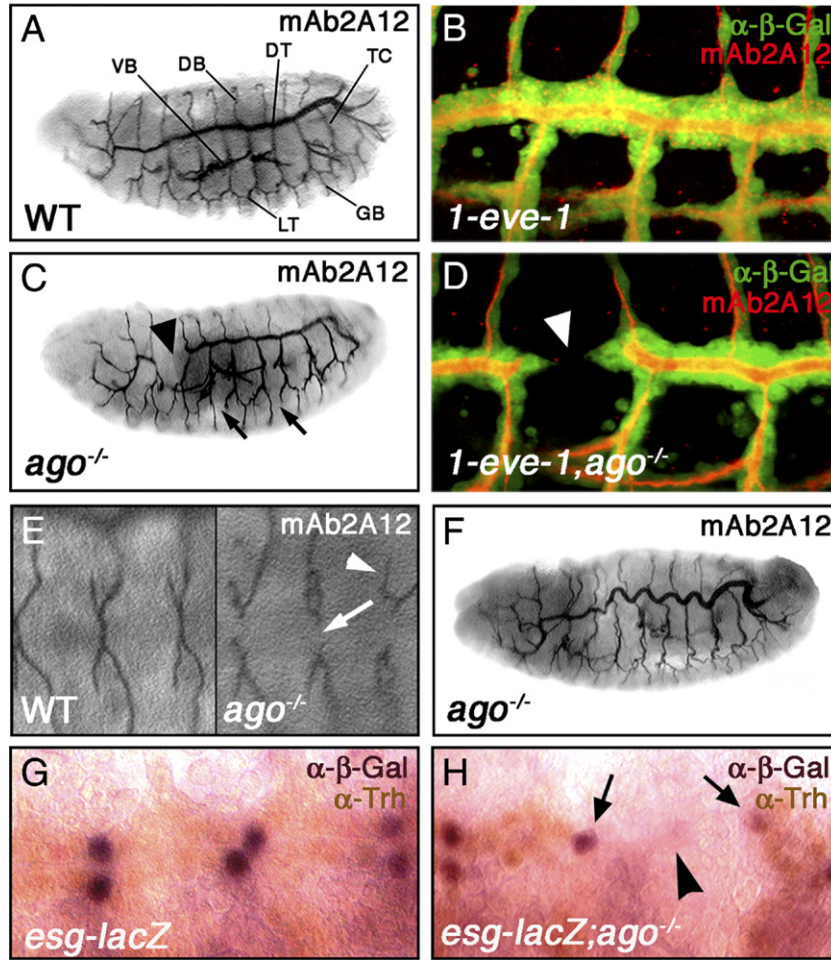
Fig. 2. *ago* is required for tracheogenesis. Lateral views of *FRT80B* (A) or *ago* embryos (C, F) stained with mAb2A12 to visualize the tracheal. Major tracheal branches are indicated in panel A: dorsal trunk (DT), lateral trunk (LT), transverse connectives (TC), dorsal branches (DB), ganglionic branches (GB), and visceral branches (VB). *ago* mutants display interruptions in the lumen of the DT (arrowhead in panel C) and LT (arrows in panel C). *1-eve-1* (B) or *1-eve-1, ago* (D) embryos stained with anti-β-Gal (green) to mark tracheal cells and mAb2A12 to mark the lumen (red). The DT lumen interruptions in *ago* mutant embryos correspond to physical breaks in the DT (arrowhead in panel D). Dorsal views of *FRT80B* (E, left panel) and *ago* (E, right panel) embryos stained with mAb2A12. *ago* mutant embryos show defects in DB fusion (arrow) as well as DB misrouting (arrowhead). The DT lumens in *ago* mutant embryos display a convolution defect (F). Staining of *esg-lacZ* (G) and *esg-lacZ;ago* (H) embryos with anti-Trh (brown) and anti-β-Gal (purple). Arrows in H mark fusion cells in adjacent placodes. Arrowhead indicates a break in the dorsal trunk. Panels B and D are reconstructions of serial sections.

embryos. The first of these is interruptions, or 'breaks', in the continuity of the tracheal lumen (Figs. 2C–E). The breaks occur throughout the tracheal system and are prominent in the dorsal trunk (DT; Figs. 2C, D, arrowheads), the lateral truck (LT; Fig. 2C, arrows), and between dorsal branches of opposing tracheal placodes (DB; Fig. 2E, arrow). What appears to be a misrouting phenotype is also observed in the dorsal branches (Fig. 2E, arrowhead) and ganglionic branches (data not shown). Approximately 70% of all *ago* mutant embryos show combinations of these break or misrouting effects. The second prominent tracheal phenotype (occurring in ∼25% of all *ago* mutant embryos) is excess lumen convolution throughout the primary and secondary branches (Fig. 2F). This combined spectrum of breaks, apparent misrouting, and convolution indicates that *ago* is required for normal development of the tracheal system. Moreover, the absence of any accompanying defects in the major morphogenetic events of embryogenesis (NTM and KHM, unpublished) suggests that these phenotypes reflect

a requirement for *ago* in the trachea, rather than as a secondary effect of a more general developmental role outside this tissue.

The DT break phenotype occurs in almost half of all *ago* mutant embryos (46%, $n=85$) with an average of 1.2 ± 0.09 breaks among those that show the phenotype ($n=39$). On a per fusion event basis, this corresponds to a greater than 15-fold increase in the rate of defective interplacode fusion events in *ago* mutants compared to control embryos (Supplemental Fig. 1). Due to the prevalence of this phenotype, DT morphogenesis was selected as a system in which to characterize the role of *ago* in the developing tracheal system. To investigate the cellular architecture of DT breaks in *ago* mutant embryos, the *1-eve-1* enhancer trap line, which carries a *lacZ* insertion in the *trh* gene and expresses β-galactosidase (β-gal) in every tracheal cell (Perrimon et al., 1991; Wilk et al., 1996), was placed in the wild type and *ago* mutant backgrounds (Figs. 2B, D). Anti-β-gal staining of these embryos reveals that lumenal gaps detected

with the mAb2A12 antibody reflect physical gaps between cells of adjacent tracheal placodes (Fig. 2D, arrowhead). Interplacode fusion along the DT is normally dependent upon specialized 'fusion cells', which are specified 2 per placode by a *Notch*-dependent process (Ikeya and Hayashi, 1999). At the appropriate stage, one migrates anteriorly and the other posteriorly to meet with fusion cells coming from adjacent placodes. Thus, the gaps between adjacent DT placodes in *ago* mutant embryos suggest either that *ago* is necessary for proper fusion cell specification, or that *ago* mutations impair fusion cell migration and/or fusion. To test these hypotheses, DT fusion cells were visualized in wild type and *ago* mutant stage 15 embryos (Figs. 2G, H) using the fusion cell-specific enhancer trap *escargot* (*esg*)-*lacZ* (Tanaka-Matakatsu et al., 1996). Analysis of wild type embryos in which the process of DT fusion is complete shows *esg-lacZ* expression (purple nuclei; Fig. 2G) in a pair of adjacent fusion cell nuclei. In *ago* mutant embryos, pairs of *esg-lacZ* positive fusion cells flank regions of DT breaks (Fig. 2H, arrows mark fusion cell nuclei, arrowhead marks gap in DT). Analysis of a second fusion cell marker, the Dysfusion protein (Jiang and Crews, 2003), gives similar results (data not shown). Thus *ago* DT breaks are not associated with altered fusion cell numbers but rather a failure of *ago* mutant DT fusion cells to fuse with adjacent placodes. This differs significantly from tracheal phenotypes elicited by *btlGal4*-driven over-expression the putative Ago target Notch (Fryer et al., 2004; Gupta-Rossi et al., 2001; Oberg et al., 2001; Tsunematsu et al.,

2004; Wu et al., 2001), which results in a complete loss of fusion cells (Ikeya and Hayashi, 1999). The lack of an effect on fusion cell number also contrasts with *ago* proliferative phenotypes in imaginal discs (Moberg et al., 2001, 2004). To further confirm this, we measured total cell number in wild type and *ago* mutant DTs using an anti-Tango antiserum (Sonnenfeld et al., 1997). This analysis shows that these genotypes have approximately equal numbers of nuclei per DT segment ($wt = 16.7 \pm 0.4$, $n = 6$; $ago = 17.0 \pm 0.7$, $n = 9$). Thus, the primary effect of *ago* loss in the DT is not on cell number, but rather on the ability of cells to follow the normal developmental program of cell migration and fusion.

Because Ago protein is expressed uniformly in tracheal and non-tracheal cells (Supplemental Fig. 1), the requirement for *ago* in the DT could be indicative of a cell-autonomous role for *ago* in tracheal cells or it might reflect a non-cell autonomous role for *ago* outside the developing placode in, for example, the mesodermal 'bridge cells' necessary for DT fusion (Wolf and Schuh, 2000). To determine the site of *ago* action, a wild type *UAS-ago* transgene and a dominant-negative *UAS-agoΔF* transgene were expressed specifically in the developing tracheal system using the *btl-Gal4* driver (Shiga et al., 1996). *btl-Gal4*-driven expression of wild type *ago* in an ago^1/ago^3 mutant background significantly reduces the frequency of DT breaks (Fig. 3E, compare yellow and blue bars) and the other observed tracheal phenotypes in *ago* mutant embryos (data not shown). Moreover, *btl-Gal4*-driven expres-
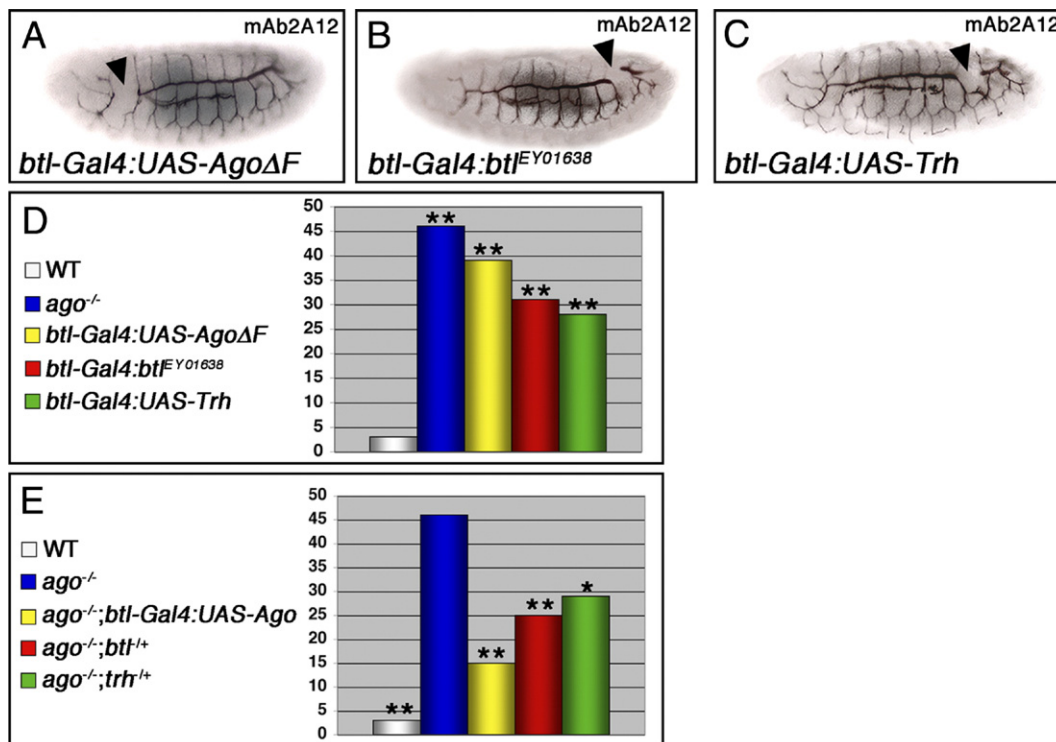

Fig. 3. *ago* acts within tracheal cells and interacts with Btl/FGF signaling components. mAb2A12 staining of stage 15 embryos (A–C). *btl-Gal4*-driven expression of *agoΔF* (A), *btl* (B), or *trh* (C) phenocopies the *ago* DT break phenotype (arrowheads). (D, E) Quantitative summary of the DT break phenotype in stage 15 embryos of the indicated genotypes. (D) *btl-Gal4*-driven expression of *agoΔF* (yellow), *btl* (red), or *trh* (green) phenocopies *ago* mutations (blue). (E) The *ago* mutant phenotype is suppressed by expression of wild type *ago* in the *btl-Gal4* domain (yellow), or by reducing the genetic dosage of either *btl* (red) or *trh* (green). *$p < 0.05$ and **$p < 0.01$ compared to *FRT80B* (D) or *ago* (E).

sion of the *agoΔF* dominant-negative transgene in otherwise wild type tracheal cells is sufficient to produce DT breaks at similar penetrance as zygotic deficiency for *ago* (Table 2 and Figs. 3A, D). The *agoΔF* allele carries an internal deletion of the core F-box domain (Moberg et al., 2004), and is defective in ubiquitin-dependent protein degradation. While these data do not rule out a secondary role for *ago* in non-tracheal cells, they do argue that *ago* plays a required role in a protein degradation pathway that is active in embryonic tracheal cells.

ago acts upstream of trachealess and breathless

Because loss of *ago* leads to excess activity of proteins normally regulated by Ago-dependent degradation (Moberg et al., 2001, 2004), known Ago target proteins were tested for their ability to reproduce *ago* mutant tracheal phenotypes when expressed in the *btl-Gal4* domain. Expression of *cycE* and *dMyc*, two targets of Ago in imaginal disc cells, does not reproduce the *ago* mutant tracheal phenotype (Table 2), suggesting that *ago* controls tracheal morphogenesis via a novel target. Significantly, *btl-Gal4*-driven expression of either *trh* or its downstream target *btl* produces DT breaks of similar penetrance and expressivity as *ago* mutations (Figs. 3B–D), and also leads to lumen convolution (data not shown). Moreover, loss-of-function alleles of *trh* (*trh^10512*; Isaac and Andrew, 1996) or *btl* (*btl^dev1*; Kennison and Tamkun, 1988) are each able to dominantly suppress *ago* tracheal phenotypes (Fig. 3E, green and red bars, respectively). The sensitivity of *ago* phenotypes to the genetic dosage of *trh* and *btl* suggests that *ago* may inhibit Trh in the developing trachea. To test the effect *ago* mutations on Trh protein levels, wild type and *ago* mutant embryos were stained with a Trh-specific antiserum (Fig. 4). Compared to control embryos, *ago* mutant embryos contain significantly higher levels of Trh in all tracheal cells (Figs. 4A, B). This effect is also evident in immunoblot blot analysis of Trh levels in *ago* and control embryos (Fig. 4C). Trh protein is normally detected in the nuclei of all tracheal cells, but is specifically eliminated from fusion cells, including those of the dorsal trunk, by a mechanism that requires fusion-cell-specific expression of the Dysfusion (Dys) bHLH-PAS domain transcription factor (Jiang and Crews, 2003). In addition to limiting the steady-state levels of Trh in all tracheal cells, *ago* is also required for the Dys-stimulated elimination of Trh that

occurs specifically in fusion cells (Figs. 4D, E). Expression of Dys occurs normally in *ago* embryos (see middle panel, Fig. 4E), but in these same cells Trh levels do not decline, and DT fusion cells with high levels of both Dys and Trh are readily observed (Fig. 4E, arrows). Thus, the antagonistic genetic interaction between *ago* and *trh* in the tracheal system appears to have its basis in a requirement for *ago* in limiting the steady-state levels of Trh in all tracheal cells, and in the specific elimination of Trh from fusion cells.

The effect of *ago* alleles on Trh levels, and the genetic interaction between *ago* and the Trh target gene *btl*, indicates that ectopic Trh-driven transcription of *btl* may contribute to the *ago* phenotype. The developmental regulation of the *btl* promoter is complex and involves inputs from a number of factors other than Trh, including the transcriptional activators *pointed* (Klambt, 1993; Ohshiro et al., 2002) and *ventral veinless* (Anderson et al., 1996), and the transcriptional repressors *anterior open* (Ohshiro et al., 2002) and *spalt* (Kuhnlein and Schuh, 1996). To test whether the failure to down-regulate Trh in *ago* mutant cells is sufficient to cause misexpression of *btl*, RNA *in situ* hybridization analysis was performed using a *btl*-specific anti-sense RNA probe. In stage 15 control embryos, levels of *btl* mRNA expression in the DT do not rise above the background signal obtained with *btl* anti-sense (Fig. 5A) or sense (data not shown) probes. In contrast, pairs of *btl*-positive cells are evident along the DT of all *ago* mutant embryos (Fig. 5B, see arrows). The location and pattern of this ectopic *btl* expression suggest that these paired cells correspond to fusion cells, and that failure to eliminate Trh in these cells leads to ectopic *btl* transcription. The lack of a similar effect in the remaining *ago* mutant tracheal cells suggests that excess Trh must collaborate with fusion-cell-specific factors in order to drive ectopic *btl* transcription.

In view of the requirement for *btl* in the *ago* phenotype (see Table 3 and Fig. 3B) and the finding that excess Btl activity disrupts DT architecture (see Fig. 3B and Dammai et al., 2003; Lee et al., 1996; Ohshiro et al., 2002), the effect of *ago* on *btl* suggests that Trh-driven transcriptional deregulation of *btl* is an important element of *ago* DT phenotype. However, while the molecular effect of *ago* inactivation on Trh and *btl* is fully penetrant, the resultant morphological defects in tracheal structure are not. This might be expected if the elevated levels of Trh and *btl* reach a threshold that is sufficient to perturb tracheal development in a portion of embryos, but that other pathways acting redundantly to *ago* are able to enforce the developmental down-regulation of the Btl pathway. If so, then *ago* mutations might be predicted to sensitize the tracheal system to other mutations that increase Btl activity by non-transcriptional mechanisms. To test this, a loss-of-function allele of the *abnormal wing discs* gene (*awd^j2A4*; Spradling et al., 1999), which encodes a factor that promotes the endocytic down-regulation of the Btl receptor in embryonic tracheal cells (Dammai et al., 2003), was assayed for its ability to enhance the *ago* tracheal phenotype (Figs. 5C, D). Reducing *awd* gene dosage by half in *ago* mutant animals strongly enhances both the penetrance (from 46% of embryos to greater than 80% of embryos; see Fig. 5D, Table 4, and Supplemental Fig. 1) of the

Table 2
ago is phenocopied by ectopic expression of FGF pathway members, but not the Ago targets Cyclin E and dMyc

Genotype	DT breaks (%)	n=
FRT80B	3 [a]	61
ago^1/ago^3	46	85
btl-Gal4:UAS-agoΔF	39	56
btl-Gal4:UAS-trh	28	56
btl-Gal4:btl^EY01638	31	53
btl-Gal4:UAS-CycE	18 [a]	64
btl-Gal4:UAS-dMyc	3 [a]	66

Percent penetrance of the dorsal trunk 'break' phenotype in embryos of the indicated genotypes.
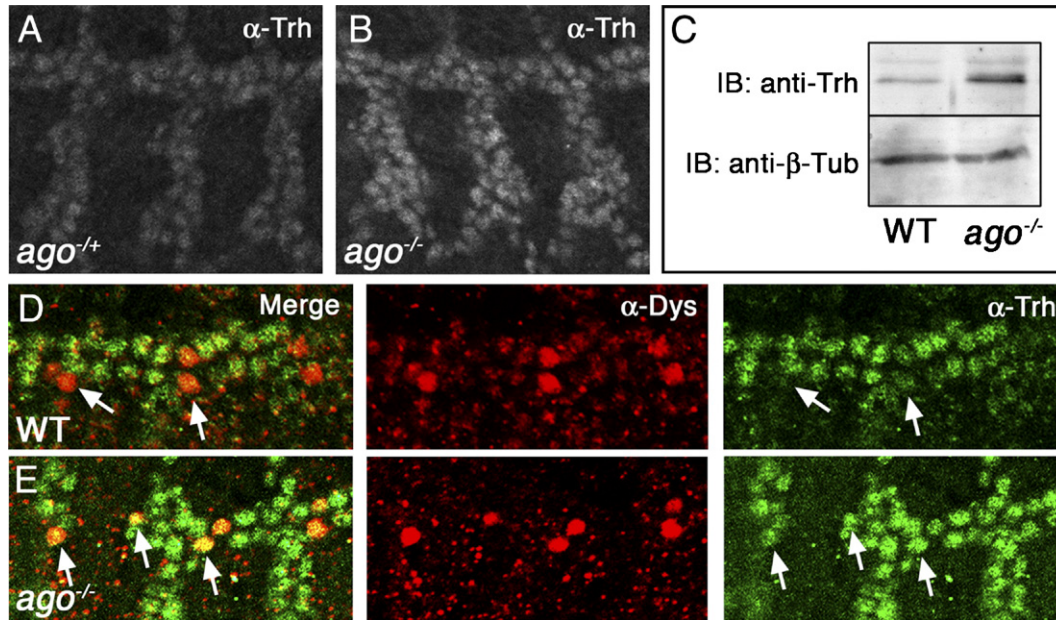
[a] $p < 0.01$ compared to *ago^1/3*.

Fig. 4. *ago* regulates Trh levels and is required for Trh elimination in tracheal fusion cells. Anti-Trh staining in *ago/TM6B, P{iab-2(1.7)lacZ}6B, Tb*[1] (A) and *ago*[1]/ *ago*[3] (B) embryos. (C) Anti-Trh (top) and anti-β-tub (bottom; loading control) Western blot analysis of stage 13/14 control and *ago* mutant embryos (10 embryos/ lane). *FRT80B* (D) and *ago* (E) embryos stained with anti-Trh (green, right panel) and anti-Dys (red, center panel) to mark fusion cells. Trh levels are reduced in Dys-positive wild type fusion cells (arrows in panel D), but not in Dys-positive *ago* mutant fusion cells (arrows in panel E).

DT break phenotype and its expressivity among affected embryos (from 1.2 ± 0.09 breaks/embryo, $n=39$ to 6.1 ± 0.95 breaks/embryo, $n=41$). These *ago/ago,awd/+* embryos also show a much more severe disruption of the entire tracheal system than do *ago* mutants alone (compare Figs. 5C to 2C). Moreover, a significant fraction of *ago/+,awd/+ trans*-hetero-zygous embryos show DT breaks. In view of the data indicating that *ago* and *awd* are both upstream of *btl* via transcriptional and endocytic mechanisms, respectively, these strong synthetic effects suggest that *ago* and *awd* mutations collaborate to deregulate Btl in the developing tracheal system.

Ago binds Trh and restricts Trh levels in cells

The ability of *ago* mutations to elevate Trh levels in vivo and to uncouple Trh levels from the rise in Dys indicates that Ago acts downstream of Dys as part of the mechanism that eliminates Trh protein in fusion cells. To examine interactions between Ago and Trh more closely, epitope tagged versions of these proteins were co-expressed in S2 cells (Figs. 6A, B). Analysis shows that while Trh accumulates to high levels when expressed in S2 cells, co-expression of Ago results in a subtle but reproducible reduction ($\sim$20% by density quantitation; Photoshop) in Trh levels (Fig. 6A, top panel, lanes 1–2). This effect appears to parallel the negative effect *ago* has on Trh levels in non-fusion cells that do not normally express Dys (see Fig. 4B). However, when Ago and Trh are co-expressed with Dys, the in vivo trigger of Trh down-regulation, Trh levels drop dramatically (Fig. 6A, top panel, lane 3) in much the same way Trh levels drop in response to Dys expression in vivo (see Fig. 4D and in Jiang and Crews, 2003). The parallel decline in the level of Ago is consistent with findings that other F-box

proteins are destabilized by reductions in the level of their substrates (Li et al., 2004) and mimics the relationship between dMyc and Ago stability in S2 cells (Moberg et al., 2004). Examination of the effect of Dys on Trh reveals that expression of *dys* is sufficient to decrease Trh levels in the absence of exogenous Ago (Fig. 6B, lane 3). However, as is observed in embryonic tracheal cells (Fig. 4E), this effect of Dys in S2 cells still requires endogenous Ago since RNAi-knockdown of *ago* is sufficient to block it (Fig. 6B, lane 4). Addition of the proteasome inhibitor MG132 also blocks the Ago/Dys-stimulated decline in Trh levels in S2 cells (Fig. 6B, lane 5). In parallel to these in vitro effects, *btl-Gal4*-mediated expression of dominant-negative alleles of the proteasome subunits *Pros26* and *Prosβ2* (Belote and Fortier, 2002) is sufficient to phenocopy *ago* alleles and block down-regulation of Trh in embryonic fusion cells (Fig. 6C). From these data, it appears that Trh is a target of a proteasomal degradation pathway in embryonic tracheal cells and in cultured S2 cells, and that in both cases the mechanism underlying this effect requires *ago* and can be greatly potentiated by co-expression of *dys*.

The genetic and functional interactions between *ago* and *trh* suggest that their encoded products may physically interact in cells. To test this hypothesis, Flag-tagged Trh and HA-tagged versions of either wild type Ago, the AgoΔF dominant negative protein, or the truncated Ago[1] protein (lacking an intact WD domain) were expressed in S2 cells and analyzed by co-immunoprecipitation (Fig. 7). Wild type Ago, Ago[1], and AgoΔF are all recovered in anti-Flag immunoprecipitates (Fig. 7A, lanes 2–4) and reciprocally, Flag-Trh is readily detected in anti-HA immunoprecipitates from cells expressing HA-AgoΔF (Fig. 7B). Thus, in the absence of exogenous Dys, Trh is able to interact with all three forms of Ago in S2 cells,
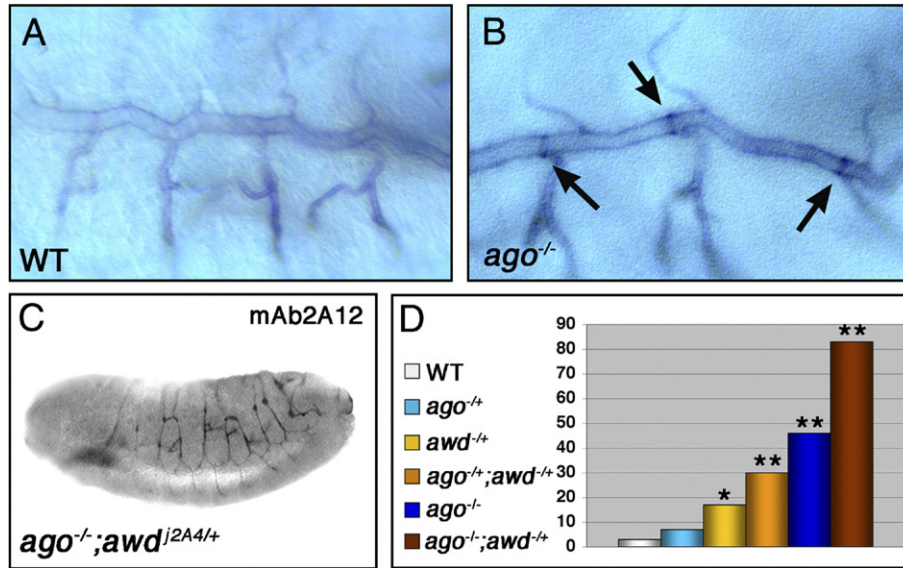
Fig. 5. *btl* transcription is deregulated in *ago* mutant embryos. RNA in situ hybridization of *FRT80B* (A) and *ago* (B) stage 16 embryos with *btl* anti-sense probe. Arrows in B denote *btl*-expressing cells. (C) Lateral view of a stage 15 *ago;awd*^{−/+} embryo stained with mAb2A12 showing enhanced expressivity of the *ago* mutant phenotype. (D) Quantitative summary of the DT break phenotype in stage 15 embryos of the indicated genotypes showing interactions between *ago* and *awd*.

including the Ago[1] WD-truncation mutant that is defective in Trh regulation in vivo. Co-expression of Dys with these combinations of Ago and Trh, and simultaneously blocking proteasome function so as to stabilize the Ago–Trh complex, induces a significant change the nature of the Ago–Trh interaction (Fig. 7C). The form of Trh protein that accumulates in MG132-treated, Dys-expressing cells remains competent to bind wild type Ago but fails to interact with the WD-truncation mutant Ago[1] (Fig. 7C, top panel, compare lanes 3 and 5). Thus, an *ago* mutation that deregulates Trh levels in vivo is defective in binding to the form of Trh normally targeted for proteasome-dependent elimination in Dys-expressing fusion cells. Considered together, these data show that Ago and Trh can bind specifically to one another, and that this interaction is required to limit Trh levels in vivo.

Discussion

The biological properties of individual F-box proteins are to a large degree determined by their repertoire of target proteins. In the case of the *Drosophila* Ago F-box protein, failure to degrade these targets promotes excess proliferation of imaginal

disc cells. This observation has led to the identification of Cyclin E and Myc proteins as *ago* targets (Moberg et al., 2001, 2004). However, the broad pattern of Ago expression in the embryo suggests that it might regulate distinct processes and targets in other cell types. In view of the rapidly growing body of work showing that inactivation of human *ago*/Fbw7 is a common event in a variety of cancers (e.g. Malyukova et al., 2007; O'Neil et al., 2007; Thompson et al., 2007), identification of these targets may provide important insight into the biology of cancers lacking *ago* function.

Here we show that *Drosophila* Ago is required for the post-mitotic morphogenesis of the embryonic tracheal system and that this requirement is due, at least in part, to the ability of Ago to bind directly to a previously unrecognized target, the Trh transcription factor, and stimulate its proteasomal degradation. This *ago* degradation mechanism appears to fulfill different regulatory roles in different populations of tracheal cells. In non-fusion tracheal cells, *ago* is required to limit overall levels of Trh, which is normally expressed at moderate levels throughout the tracheal system. In tracheal fusion cells, the *ago* degradation mechanism appears to be strongly potentiated by an unidentified signal generated by Dys, such that Trh is completely eliminated from Dys-expressing cells.

Table 3
The *ago* phenotype is dominantly suppressed by alleles of FGF pathway members, and is rescued by tracheal-cell-specific expression of Ago

Genotype	DT breaks (%)	n=
FRT80B	3**	61
ago¹/ago³	46	85
ago¹/ago³;btl-Gal4:UAS-ago	15**	73
ago¹/ago³;trh¹⁰⁵¹²/+	31*	135
ago¹/ago³;btl^dev1/+	26**	99

Percent penetrance of the dorsal trunk 'break' phenotype in embryos of the indicated genotypes. *p<0.05 and **p<0.01 compared to *ago^1/3*.

Table 4
ago dominantly interacts with an allele of the Btl antagonist *awd*

Genotype	DT breaks (%)	n=
FRT80B	3	61
ago³/+	7	56
awd^j2A4/+	17*	42
ago³,awd^j2A4/+	30**	33
ago³,awd^j2A4/ago¹	83**	52

Penetrance of indicated phenotypes in embryos of the indicated genotypes. *p<0.05 and **p<0.01 compared to *FRT80B*.
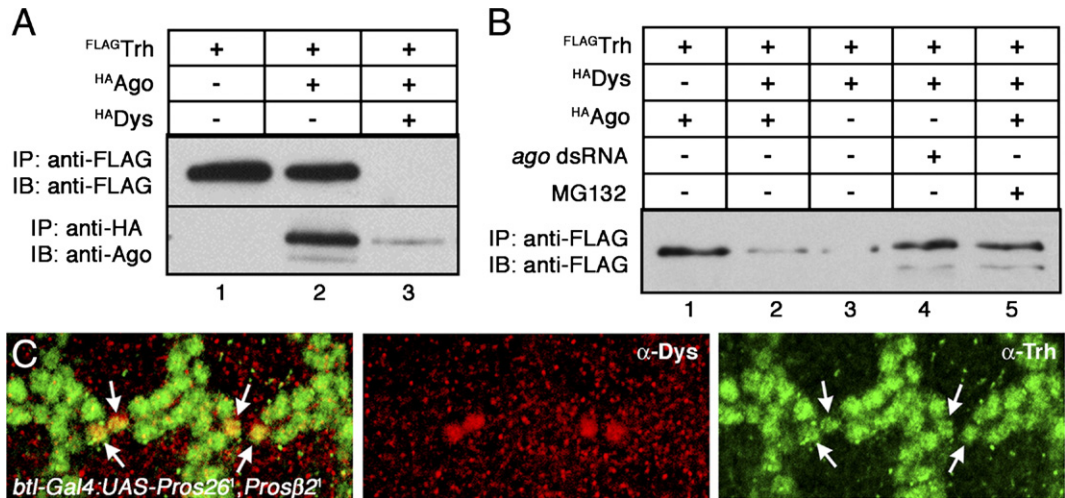
Fig. 6. Ago regulates Trh levels in S2 cells and during embryogenesis. Quantification of the steady-state levels of either Trh and Ago by immunoprecipitation-immunoblot (IP/IB) from S2 cells transfected with the indicated plasmids. (A) Trh accumulate to detectable levels in S2 cells (lane 1), are slightly reduced in the presence of Ago (lane 2), and are greatly reduced after co-expression of Ago and Dys (lane 3). (B) The Dys-mediated reduction in Trh levels occurs in the absence of transfected Ago (lane 3) but is blocked by *ago* dsRNA treatment (lane 4) or by blocking proteasome function with MG-132 (lane 5). (C) Inhibition of proteasome function also stabilizes Trh levels *in vivo*. *btl-Gal4:UAS-Pros26[1],UAS-Prosβ2[1]* embryos stained with anti-Trh (green, right panel) and anti-Dys (red, center panel) show a failure to down-regulate Trh levels in fusion cells (arrows).

At a genetic level, the dependence of *ago* tracheal phenotypes on *trh* gene dosage argues that that elevated Trh levels are primarily responsible for branching defects that occur in *ago* zygotic mutant embryos. In support of this, persistent Trh expression is also observed in *ago* mutant fusion cells in other tracheal branches (NTM and KHM, unpublished observation). This novel role for Ago in tracheal development is supported by the independent finding that homozygosity for a genomic deletion containing the *ago* locus is associated with cell

migration defects in embryonic tracheal metameres (Myat et al., 2005).

Many important developmental events are controlled by multiple mechanisms that collaborate to regulate a key step in the process. This somewhat redundant control insulates the process from defects in any single pathway, such that major defects only occur when multiple control mechanisms are blocked. The observation that the effect of *ago* mutations on Trh and *btl* levels is completely penetrant, but the resulting
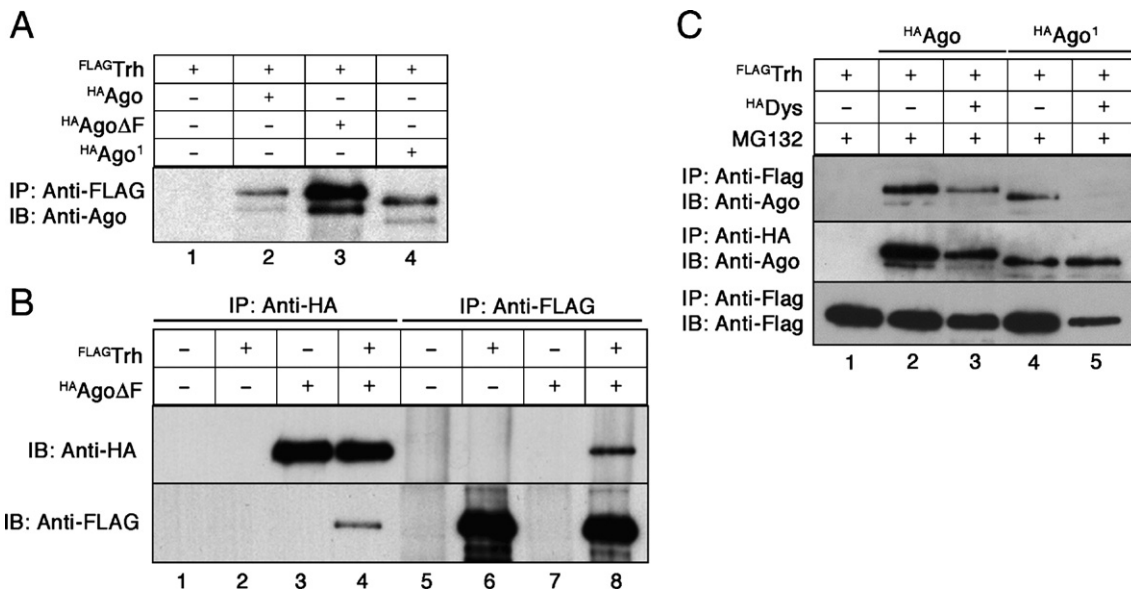

Fig. 7. Physical interaction between Ago and Trh. IP/IB analysis from S2 cells expressing the indicated cDNAs shows that wild type Ago, AgoΔF, and Ago[1] are recovered in anti-Flag precipitates (A) and that Trh is reciprocally recovered in anti-HA precipitates from cells expressing AgoΔF (B). IP/IB analysis of MG132-treated cells expressing the indicated cDNAs (C) shows that Trh is bound equally well by Ago (top panel, lane 2) and Ago[1] (top panel, lane 4) in the absence of Dys, but that in Dys-positive cells Trh is bound only by wild type Ago (top panel, lane 3) but not the Ago[1] mutant (top panel, lane 5) that is defective in Trh regulation in vivo. Loading controls for Ago (middle panel) and Trh (bottom panel) are shown.

morphological defects are not, suggests that another pathway acts redundantly to *ago* to control tracheal development. The strong, dominant enhancement of the *ago* phenotype by a mutation in the *awd* gene fits very well into a model in which multiple pathways are responsible for the precisely timed down-regulation of the Breathless/FGF pathway: *ago* attenuates *btl* transcription by degrading Trh, *awd* lowers levels of Btl protein on the cell surface by promoting its endocytic internalization (Dammai et al., 2003), and other pathways act independently to control expression of the FGF ligand *branchless* in non-tracheal cells (Merabet et al., 2005; Sutherland et al., 1996). Thus, the incomplete penetrance of the *ago* phenotype is not indicative of an insignificant role for the gene in tracheal development, but rather may indicate that the tracheal system uses multiple mechanisms to redundantly control a key step in its development.

The Ago WD repeat region binds Cyclin E and dMyc, and the current work demonstrates that it also binds Trh. Broadly, the Ago–Trh interaction is quite similar to interactions with Cyclin E and dMyc: it is required for the down-regulation of substrate levels in vivo, and its disruption elevates levels of substrate that then drive downstream phenotypes. For substrates like Myc, site-specific phosphorylation generates a motif that binds to the Ago WD-region and stimulates rapid, SCF-mediated protein turnover of the target protein (reviewed in Minella and Clurman, 2005). In contrast, the data here suggest that Trh can physically interact with Ago in two distinct configurations: one that does not require an intact WD-domain and a second WD-dependent mode of binding. The observation that the Ago[1] allele can participate in the first complex but not the second and is defective in Trh regulation in vivo, suggests that like other Ago targets, WD-dependent binding is associated with rapid Trh turnover. Expression of Dys appears to shift the balance in favor of this second mode of binding. Combined with the genetic and phenotypic data implicating *ago* as an in vivo regulator of Trh activity, these molecular data support a model in which Ago can bind to Trh in the absence of Dys and inefficiently stimulate Trh turnover by a WD-dependent mechanism. This inefficient mechanism may be responsible for the fairly mild increase in Trh levels observed in all *ago* mutant dorsal trunk cells. However, in the presence of Dys, the efficiency of Trh turnover in DT fusion cells is enhanced to the degree that the entire pool of Trh is rapidly eliminated. Interestingly, the correlate of this hypothesis – that ectopic expression of *dys* in non-fusion cells should be sufficient to trigger down-regulation of endogenous Trh – was confirmed in a recent study (Jiang and Crews, 2006).

The nature of the Dys-generated signal responsible for this effect is not currently known. Precedent with other Ago targets suggests that it may involve Trh phosphorylation (Fryer et al., 2004; Koepp et al., 2001; Nateri et al., 2004; Sundqvist et al., 2005; Wei et al., 2005; Welcker et al., 2003, 2004; Yada et al., 2004; Ye et al., 2004). Recent work on the mammalian *ago* ortholog Fbw7 has shown that interactions with substrates can also be modulated by interaction with accessory factors (Punga et al., 2006), or by conformational changes in the substrate driven by the isomerization of proline residues within the Ago/ Fbw7 binding motif (van Drogen et al., 2006). Proline isomerization has been implicated in the degradation of mammalian c-Myc (Yeh et al., 2004), but such mechanisms are not currently known to play a role in the degradation of either Myc or bHLH-PAS proteins in *Drosophila*. An important goal of future studies will be to determine if any of these types of mechanisms are involved in Dys-induced Trh degradation in tracheal cells.

The requirement for *ago* in tracheal cells suggests that the consequences of *ago* loss vary considerably depending on the proliferative state of the cells, their location within the organism, and their developmental stage. *ago* mutant clones in the mitotically active larval eye disc show no evidence of excessive Trh levels or deregulated Btl/FGF signaling (NTM and KHM, unpublished) and conversely, *ago* zygotic mutant trachea do not display 'extra cell' defects similar to those observed in the eye. The origins of this tissue specificity are currently not clear, although it might simply reflect the differential expression patterns of Ago targets in various mitotic and post-mitotic cell populations. There is currently no evidence that the mammalian Trh homologs NPAS-1 and NPAS-3 are degraded by an Ago/Fbw7-dependent mechanism in mammalian cells. However, the finding that *Fbw7* knock-out mouse embryos display defects in vascular development (Tetzlaff et al., 2004; Tsunematsu et al., 2004) seems to indicate that the Fbw7 ligase may also target proteins involved in tubular morphogenesis, and intriguingly both NPAS1 and NPAS3 have been linked either to this process (Levesque et al., 2007) or to the transcriptional control of FGFR genes (Pieper et al., 2005). It has been suggested that the *Fbw7* vascular defects arise due to Notch misregulation. However, since FGF signaling is known to control branching morphogenesis of the mammalian vasculature and lung (Min et al., 1998; Walgenbach et al., 1995), the data presented here raise the possibility that vascular phenotypes in *Fbw7* knock-out mouse embryos may also reflect the deregulation of developmental pathways that control branching morphogenesis via mammalian homologs of *trh* and *btl*.

Acknowledgments

Appendix A. Supplementary data

Supplementary data associated with this article can be found, in the online version, at doi:10.1016/j.ydbio.2007.10.002.

References

Anderson, M.G., Certel, S.J., Certel, K., Lee, T., Montell, D.J., Johnson, W.A., 1996. Function of the *Drosophila* POU domain transcription factor drifter as an upstream regulator of breathless receptor tyrosine kinase expression in developing trachea. Development 122, 4169–4178.

Balakrishnan, A., Bleeker, F.E., Lamba, S., Rodolfo, M., Daniotti, M., Scarpa, A., van Tilborg, A.A., Leenstra, S., Zanon, C., Bardelli, A., 2007. Novel somatic and germline mutations in cancer candidate genes in glioblastoma, melanoma, and pancreatic carcinoma. Cancer Res. 67, 3545–3550.

Belote, J.M., Fortier, E., 2002. Targeted expression of dominant negative proteasome mutants in *Drosophila melanogaster*. Genesis 34, 80–82.

Brand, A.H., Perrimon, N., 1993. Targeted gene expression as a means of altering cell fates and generating dominant phenotypes. Development 118, 401–415.

Bredel, M., Bredel, C., Juric, D., Harsh, G.R., Vogel, H., Recht, L.D., Sikic, B.I., 2005. Functional network analysis reveals extended gliomagenesis pathway maps and three novel MYC-interacting genes in human gliomas. Cancer Res. 65, 8679–8689.

Brunskill, E.W., Witte, D.P., Shreiner, A.B., Potter, S.S., 1999. Characterization of npas3, a novel basic helix–loop–helix PAS gene expressed in the developing mouse nervous system. Mech. Dev. 88, 237–241.

Cabernard, C., Affolter, M., 2005. Distinct roles for two receptor tyrosine kinases in epithelial branching morphogenesis in *Drosophila*. Dev. Cell 9, 831–842.

Calhoun, E.S., Jones, J.B., Ashfaq, R., Adsay, V., Baker, S.J., Valentine, V., Hempen, P.M., Hilgers, W., Yeo, C.J., Hruban, R.H., Kern, S.E., 2003. BRAF and FBXW7 (CDC4, FBW7, AGO, SEL10) mutations in distinct subsets of pancreatic cancer: potential therapeutic targets. Am. J. Pathol. 163, 1255–1260.

Dammai, V., Adryan, B., Lavenburg, K.R., Hsu, T., 2003. *Drosophila* awd, the homolog of human nm23, regulates FGF receptor levels and functions synergistically with shi/dynamin during tracheal development. Genes Dev. 17, 2812–2824.

Fryer, C.J., White, J.B., Jones, K.A., 2004. Mastermind recruits CycC:CDK8 to phosphorylate the Notch ICD and coordinate activation with turnover. Mol. Cell 16, 509–520.

Ghabrial, A., Luschnig, S., Metzstein, M.M., Krasnow, M.A., 2003. Branching morphogenesis of the *Drosophila* tracheal system. Annu. Rev. Cell Dev. Biol. 19, 623–647.

Gupta-Rossi, N., Le Bail, O., Gonen, H., Brou, C., Logeat, F., Six, E., Ciechanover, A., Israel, A., 2001. Functional interaction between SEL-10, an F-box protein, and the nuclear form of activated Notch1 receptor. J. Biol. Chem. 276, 34371–34378.

Hagedorn, M., Delugin, M., Abraldes, I., Allain, N., Belaud-Rotureau, M.A., Turmo, M., Prigent, C., Loiseau, H., Bikfalvi, A., Javerzat, S., 2007. FBXW7/hCDC4 controls glioma cell proliferation in vitro and is a prognostic marker for survival in glioblastoma patients. Cell Div. 2, 9.

Henderson, K.D., Isaac, D.D., Andrew, D.J., 1999. Cell fate specification in the *Drosophila* salivary gland: the integration of homeotic gene function with the DPP signaling cascade. Dev. Biol. 205, 10–21.

Ikeya, T., Hayashi, S., 1999. Interplay of Notch and FGF signaling restricts cell fate and MAPK activation in the *Drosophila* trachea. Development 126, 4455–4463.

Isaac, D.D., Andrew, D.J., 1996. Tubulogenesis in *Drosophila*: a requirement for the trachealess gene product. Genes Dev. 10, 103–117.

Jiang, L., Crews, S.T., 2003. The *Drosophila* dysfusion basic helix–loop–helix (bHLH)-PAS gene controls tracheal fusion and levels of the trachealess bHLH-PAS protein. Mol. Cell Biol. 23, 5625–5637.

Jiang, L., Crews, S.T., 2006. dysfusion transcriptional control of *Drosophila* tracheal migration, adhesion, fusion. Mol. Cell Biol. 26, 6547–6556.

Jin, J., Anthopoulos, N., Wetsch, B., Binari, R.C., Isaac, D.D., Andrew, D.J., Woodgett, J.R., Manoukian, A.S., 2001. Regulation of *Drosophila* tracheal system development by protein kinase B. Dev. Cell 1, 817–827.

Kennison, J.A., Tamkun, J.W., 1988. Dosage-dependent modifiers of polycomb and antennapedia mutations in *Drosophila*. Proc. Natl. Acad. Sci. U. S. A. 85, 8136–8140.

Klambt, C., 1993. The *Drosophila* gene pointed encodes two ETS-like proteins which are involved in the development of the midline glial cells. Development 117, 163–176.

Klambt, C., Glazer, L., Shilo, B.Z., 1992. breathless, a *Drosophila* FGF receptor homolog, is essential for migration of tracheal and specific midline glial cells. Genes Dev. 6, 1668–1678.

Koepp, D.M., Schaefer, L.K., Ye, X., Keyomarsi, K., Chu, C., Harper, J.W., Elledge, S.J., 2001. Phosphorylation-dependent ubiquitination of cyclin E by the SCFFbw7 ubiquitin ligase. Science 294, 173–177.

Kuhnlein, R.P., Schuh, R., 1996. Dual function of the region-specific homeotic gene spalt during *Drosophila* tracheal system development. Development 122, 2215–2223.

Kuo, Y.M., Jones, N., Zhou, B., Panzer, S., Larson, V., Beckendorf, S.K., 1996. Salivary duct determination in *Drosophila*: roles of the EGF receptor signalling pathway and the transcription factors fork head and trachealess. Development 122, 1909–1917.

Lee, T., Hacohen, N., Krasnow, M., Montell, D.J., 1996. Regulated Breathless receptor tyrosine kinase activity required to pattern cell migration and branching in the *Drosophila* tracheal system. Genes Dev. 10, 2912–2921.

Levesque, B.M., Zhou, S., Shan, L., Johnston, P., Kong, Y., Degan, S., Sunday, M.E., 2007. NPAS1 regulates branching morphogenesis in embryonic lung. Am. J. Respir. Cell Mol. Biol. 36, 427–434.

Li, Y., Gazdoiu, S., Pan, Z.Q., Fuchs, S.Y., 2004. Stability of homologue of Slimb F-box protein is regulated by availability of its substrate. J. Biol. Chem. 279, 11074–11080.

Lubarsky, B., Krasnow, M.A., 2003. Tube morphogenesis: making and shaping biological tubes. Cell 112, 19–28.

Malyukova, A., Dohda, T., von der Lehr, N., Akhondi, S., Corcoran, M., Heyman, M., Spruck, C., Grander, D., Lendahl, U., Sangfelt, O., 2007. The tumor suppressor gene hCDC4 is frequently mutated in human T-cell acute lymphoblastic leukemia with functional consequences for Notch signaling. Cancer Res. 67, 5611–5616.

Mao, J.H., Perez-Losada, J., Wu, D., Delrosario, R., Tsunematsu, R., Nakayama, K.I., Brown, K., Bryson, S., Balmain, A., 2004. Fbxw7/Cdc4 is a p53-dependent, haploinsufficient tumour suppressor gene. Nature 432, 775–779.

Maser, R.S., Choudhury, B., Campbell, P.J., Feng, B., Wong, K.K., Protopopov, A., O'Neil, J., Gutierrez, A., Ivanova, E., Perna, I., Lin, E., Mani, V., Jiang, S., McNamara, K., Zaghlul, S., Edkins, S., Stevens, C., Brennan, C., Martin, E.S., Wiedemeyer, R., Kabbarah, O., Nogueira, C., Histen, G., Aster, J., Mansour, M., Duke, V., Foroni, L., Fielding, A.K., Goldstone, A.H., Rowe, J.M., Wang, Y.A., Look, A.T., Stratton, M.R., Chin, L., Futreal, P.A., DePinho, R.A., 2007. Chromosomally unstable mouse tumours have genomic alterations similar to diverse human cancers. Nature 447, 966–971.

Merabet, S., Ebner, A., Affolter, M., 2005. The *Drosophila* Extradenticle and Homothorax selector proteins control branchless/FGF expression in mesodermal bridge-cells. EMBO Rep. 6, 762–768.

Metzger, R.J., Krasnow, M.A., 1999. Genetic control of branching morphogenesis. Science 284, 1635–1639.

Min, H., Danilenko, D.M., Scully, S.A., Bolon, B., Ring, B.D., Tarpley, J.E., DeRose, M., Simonet, W.S., 1998. Fgf-10 is required for both limb and lung development and exhibits striking functional similarity to *Drosophila* branchless. Genes Dev. 12, 3156–3161.

Minella, A.C., Clurman, B.E., 2005. Mechanisms of tumor suppression by the SCF(Fbw7). Cell Cycle 4, 1356–1359.

Minella, A.C., Grim, J.E., Welcker, M., Clurman, B.E., 2007. p53 and SCF (Fbw7) cooperatively restrain cyclin E-associated genome instability. Oncogene 26, 6948–6953.

Moberg, K.H., Bell, D.W., Wahrer, D.C., Haber, D.A., Hariharan, I.K., 2001. Archipelago regulates Cyclin E levels in *Drosophila* and is mutated in human cancer cell lines. Nature 413, 311–316.

Moberg, K.H., Mukherjee, A., Veraksa, A., Artavanis-Tsakonas, S., Hariharan, I.K., 2004. The *Drosophila* F box protein archipelago regulates dMyc protein levels in vivo. Curr. Biol. 14, 965–974.

Myat, M.M., Lightfoot, H., Wang, P., Andrew, D.J., 2005. A molecular link between FGF and Dpp signaling in branch-specific migration of the *Drosophila* trachea. Dev. Biol. 281, 38–52.

Nateri, A.S., Riera-Sans, L., Da Costa, C., Behrens, A., 2004. The ubiquitin ligase SCFFbw7 antagonizes apoptotic JNK signaling. Science 303, 1374–1378.

Oberg, C., Li, J., Pauley, A., Wolf, E., Gurney, M., Lendahl, U., 2001. The Notch intracellular domain is ubiquitinated and negatively regulated by the mammalian Sel-10 homolog. J. Biol. Chem. 276, 35847–35853.

Ohshiro, T., Saigo, K., 1997. Transcriptional regulation of breathless FGF receptor gene by binding of TRACHEALESS/dARNT heterodimers to three central midline elements in *Drosophila* developing trachea. Development 124, 3975–3986.

Ohshiro, T., Emori, Y., Saigo, K., 2002. Ligand-dependent activation of breathless FGF receptor gene in *Drosophila* developing trachea. Mech. Dev. 114, 3–11.

O'Neil, J., Grim, J., Strack, P., Rao, S., Tibbitts, D., Winter, C., Hardwick, J., Welcker, M., Meijerink, J.P., Pieters, R., Draetta, G., Sears, R., Clurman, B. E., Look, A.T., 2007. FBW7 mutations in leukemic cells mediate NOTCH pathway activation and resistance to {gamma}-secretase inhibitors. J. Exp. Med. 204, 1813–1824.

Perrimon, N., Noll, E., McCall, K., Brand, A., 1991. Generating lineage-specific markers to study *Drosophila* development. Dev. Genet. 12, 238–252.

Pieper, A.A., Wu, X., Han, T.W., Estill, S.J., Dang, Q., Wu, L.C., Reece-Fincanon, S., Dudley, C.A., Richardson, J.A., Brat, D.J., McKnight, S.L., 2005. The neuronal PAS domain protein 3 transcription factor controls FGF-mediated adult hippocampal neurogenesis in mice. Proc. Natl. Acad. Sci. U. S. A. 102, 14052–14057.

Punga, T., Bengoechea-Alonso, M.T., Ericsson, J., 2006. Phosphorylation and ubiquitination of the transcription factor sterol regulatory element-binding protein-1 in response to DNA binding. J. Biol. Chem. 281, 25278–25286.

Rajagopalan, H., Jallepalli, P.V., Rago, C., Velculescu, V.E., Kinzler, K.W., Vogelstein, B., Lengauer, C., 2004. Inactivation of hCDC4 can cause chromosomal instability. Nature 428, 77–81.

Samakovlis, C., Manning, G., Steneberg, P., Hacohen, N., Cantera, R., Krasnow, M.A., 1996. Genetic control of epithelial tube fusion during *Drosophila* tracheal development. Development 122, 3531–3536.

Shiga, Y., Tanaka-Matakatsu, M., Hayashi, S., 1996. A nuclear GFP/beta-galactosidase fusion protein as a marker for morphogenesis in living *Drosophila*. Dev. Growth Differ. 38, 99–106.

Sonnenfeld, M., Ward, M., Nystrom, G., Mosher, J., Stahl, S., Crews, S., 1997. The *Drosophila* tango gene encodes a bHLH-PAS protein that is orthologous to mammalian Arnt and controls CNS midline and tracheal development. Development 124, 4571–4582.

Spradling, A.C., Stern, D., Beaton, A., Rhem, E.J., Laverty, T., Mozden, N., Misra, S., Rubin, G.M., 1999. The Berkeley *Drosophila* Genome Project gene disruption project: single P-element insertions mutating 25% of vital *Drosophila* genes. Genetics 153, 135–177.

Sundqvist, A., Bengoechea-Alonso, M.T., Ye, X., Lukiyanchuk, V., Jin, J., Harper, J.W., Ericsson, J., 2005. Control of lipid metabolism by phosphorylation-dependent degradation of the SREBP family of transcription factors by SCF(Fbw7). Cell Metab. 1, 379–391.

Sutherland, D., Samakovlis, C., Krasnow, M.A., 1996. branchless encodes a *Drosophila* FGF homolog that controls tracheal cell migration and the pattern of branching. Cell 87, 1091–1101.

Tanaka-Matakatsu, M., Uemura, T., Oda, H., Takeichi, M., Hayashi, S., 1996. Cadherin-mediated cell adhesion and cell motility in *Drosophila* trachea regulated by the transcription factor Escargot. Development 122, 3697–3705.

Tautz, D., 2000. Whole mount in situ hybridization for the detection of mRNA in *Drosophila* embryos. In: Kessler, C. (Ed.), Nonradioactive Analysis of Biomolecules. Springer, New York, pp. 573–580.

Tetzlaff, M.T., Yu, W., Li, M., Zhang, P., Finegold, M., Mahon, K., Harper, J.W., Schwartz, R.J., Elledge, S.J., 2004. Defective cardiovascular development and elevated cyclin E and Notch proteins in mice lacking the Fbw7 F-box protein. Proc. Natl. Acad. Sci. U. S. A. 101, 3338–3345.

Thompson, B.J., Buonamici, S., Sulis, M.L., Palomero, T., Vilimas, T., Basso, G., Ferrando, A., Aifantis, I., 2007. The SCFFBW7 ubiquitin ligase complex as a tumor suppressor in T cell leukemia. J. Exp. Med. 204, 1825–1835.

Tsunematsu, R., Nakayama, K., Oike, Y., Nishiyama, M., Ishida, N., Hatakeyama, S., Bessho, Y., Kageyama, R., Suda, T., Nakayama, K.I., 2004. Mouse Fbw7/Sel-10/Cdc4 is required for notch degradation during vascular development. J. Biol. Chem. 279, 9417–9423.

van Drogen, F., Sangfelt, O., Malyukova, A., Matskova, L., Yeh, E., Means, A.R., Reed, S.I., 2006. Ubiquitylation of cyclin E requires the sequential function of SCF complexes containing distinct hCdc4 isoforms. Mol. Cell 23, 37–48.

Walgenbach, K.J., Gratas, C., Shestak, K.C., Becker, D., 1995. Ischaemia-induced expression of bFGF in normal skeletal muscle: a potential paracrine mechanism for mediating angiogenesis in ischaemic skeletal muscle. Nat. Med. 1, 453–459.

Wei, W., Jin, J., Schlisio, S., Harper, J.W., Kaelin Jr., W.G., 2005. The v-Jun point mutation allows c-Jun to escape GSK3-dependent recognition and destruction by the Fbw7 ubiquitin ligase. Cancer Cell 8, 25–33.

Welcker, M., Singer, J., Loeb, K.R., Grim, J., Bloecher, A., Gurien-West, M., Clurman, B.E., Roberts, J.M., 2003. Multisite phosphorylation by Cdk2 and GSK3 controls cyclin E degradation. Mol. Cell 12, 381–392.

Welcker, M., Orian, A., Jin, J., Grim, J.A., Harper, J.W., Eisenman, R.N., Clurman, B.E., 2004. The Fbw7 tumor suppressor regulates glycogen synthase kinase 3 phosphorylation-dependent c-Myc protein degradation. Proc. Natl. Acad. Sci. U. S. A. 101, 9085–9090.

Wilk, R., Weizman, I., Shilo, B.Z., 1996. trachealess encodes a bHLH-PAS protein that is an inducer of tracheal cell fates in *Drosophila*. Genes Dev. 10, 93–102.

Wolf, C., Schuh, R., 2000. Single mesodermal cells guide outgrowth of ectodermal tubular structures in *Drosophila*. Genes Dev. 14, 2140–2145.

Wu, G., Lyapina, S., Das, I., Li, J., Gurney, M., Pauley, A., Chui, I., Deshaies, R.J., Kitajewski, J., 2001. SEL-10 is an inhibitor of notch signaling that targets notch for ubiquitin-mediated protein degradation. Mol. Cell Biol. 21, 7403–7415.

Yada, M., Hatakeyama, S., Kamura, T., Nishiyama, M., Tsunematsu, R., Imaki, H., Ishida, N., Okumura, F., Nakayama, K., Nakayama, K.I., 2004. Phosphorylation-dependent degradation of c-Myc is mediated by the F-box protein Fbw7. EMBO J. 23, 2116–2125.

Ye, X., Nalepa, G., Welcker, M., Kessler, B.M., Spooner, E., Qin, J., Elledge, S.J., Clurman, B.E., Harper, J.W., 2004. Recognition of phosphodegron motifs in human cyclin E by the SCF(Fbw7) ubiquitin ligase. J. Biol. Chem. 279, 50110–50119.

Yeh, E., Cunningham, M., Arnold, H., Chasse, D., Monteith, T., Ivaldi, G., Hahn, W.C., Stukenberg, P.T., Shenolikar, S., Uchida, T., Counter, C.M., Nevins, J.R., Means, A.R., Sears, R., 2004. A signalling pathway controlling c-Myc degradation that impacts oncogenic transformation of human cells. Nat. Cell Biol. 6, 308–318.

Zhou, Y.D., Barnard, M., Tian, H., Li, X., Ring, H.Z., Francke, U., Shelton, J., Richardson, J., Russell, D.W., McKnight, S.L., 1997. Molecular characterization of two mammalian bHLH-PAS domain proteins selectively expressed in the central nervous system. Proc. Natl. Acad. Sci. U. S. A. 94, 713–718.